Additional Evidence of an Upper Tropospheric Zonal/Eddy Relationship during Winter

STEVEN W. LYONS

Texas A&M University, Department of Meteorology, College Station, Texas

18 January 1988 and 16 August 1988

ABSTRACT

A zonal wind oscillation with a period of about 15–35 days is isolated over the middle latitudes of the Northern Hemisphere during winter. A systematic relationship between the zonal winds and wind departures from zonal symmetry (eddies) is found for nine prominent zonal wind oscillation cycles taken from six 120-day winters. This zonal/eddy relationship consists of an oscillation between anomalous zonal flow and anomalous meridional flow, which is strongest across North America from 150°W to 0°.

1. Introduction

Variability in the zonally averaged winds has intrigued meteorologists for nearly half a century. Studies of the zonal winds and the "zonal index" cycle were carried out by Namias (1947), Riehl et al. (1950), La Seur (1954), Defant and Taba (1958), and numerous others, primarily for the Northern Hemisphere middle latitudes. In more recent years, these indices have included various energy parameters such as eddy and zonal kinetic and potential energy (e.g., Winston and Krueger 1961; McGuirk and Reiter 1976). Most of these studies, including a recent investigation by Kidson (1985) have found that the dominant temporal variability of midlatitude zonal winds is between about 2 weeks and 30 days, and that these fluctuations are primarily winter phenomena.

On the other hand, based on the original work of Madden and Julian (1971), there has been recent interest in the 40–50 day (or 30–60 day) tropical wind and convection cycle (e.g., Yasunari 1980; Weickmann 1983; Anderson and Rosen 1983; Krishnamurti and Subrahmanyam 1983; Lau and Chan 1985, 1986; Murakami and Nakazawa 1985; Murakami et al. 1986; Knutson and Weickmann 1987). These studies have linked the 40–50 day cycle in the tropics, subtropics and midlatitudes, and have shown that the cycle occurs year-round.

Close examination of the studies dealing with the frequency characteristics and the seasonal variability of tropical and midlatitude zonal wind cycles indicates that they may be two distinct zonal wind oscillations: viz., one primarily of tropical origin with a period of 30–60 days (dominant year-round) and one primarily of midlatitude origin with a period closer to 15–35 days (dominant in winter). This note will describe a zonal wind oscillation which fits the latter description. Wind fields will be shown which depict a relationship between a zonal wind oscillation and eddy variability in the subtropical and midlatitudes of the Northern Hemisphere during winter. The term "zonal/eddy" relationship is defined here as a simultaneous quasi-periodic fluctuation between the zonally averaged flow ($\bar{u}$) and departures from zonal symmetry (eddies). In general, this definition is synonymous with vacillation; however, the term quasi-periodic is used loosely.

Branstator (1984) addressed the zonal/eddy relationship using observed 300 mb monthly mean height fields. His observational results indicated that there is a zonal/eddy relationship in monthly mean data. Branstator's model results produced quasi-stationary waves similar to those observed (when the models were given the vorticity forcing derived from climatological January 300 mb flow). Although Branstator did not speculate on the cause of this zonal/eddy relationship, he indicated that it may be present in many previous observational studies of circulation anomalies, including past global teleconnection studies (e.g., Wallace and Gutzler 1981).

In this study, in support of Branstator's findings, additional evidence for an atmospheric zonal/eddy relationship is shown using daily wind data. Namely, an intraseasonal oscillation in the zonal mean upper tropospheric flow ($\bar{u}$) and a concurrent oscillation in the wind departures from zonal symmetry (eddies) are found.

2. Data and computational procedure

Diagnostics were performed on daily National Meteorological Center (NMC) analyses of winds available on a mercator grid at 5° long by approximately 5° lat intervals from 48.1°N to 48.1°S. A global dataset was

Corresponding author address: Steven W. Lyons, Department of Meteorology, Texas A&M University, College Station, TX 77843-3146.

not used. Here, the focus is on tropical, subtropical, and middle latitude regions, in particular $\bar{u}$ anomalies associated with the tropics and winter jet stream regions. Two-hundred mb winds are used, because this level is relatively data rich over oceanic regions and is near the level of maximum zonal wind speed. Six 120-day winters (1 November–28 February) encompassing the years 1973/74–1978/79 were examined.

First, a dominant midlatitude zonal wind index is derived, then anomalous eddy fields associated with this index are composited. The zonal wind index was obtained by computing zonally averaged winds ($\bar{u}$) each day over the six 120-day winter periods. Daily $\bar{u}$ values at each latitude were normalized by dividing them by the standard deviation of $\bar{u}$ at each latitude. Empirical orthogonal function (EOF) analysis was then applied to the six winter meridional $\bar{u}$ dataset. I focused on the intraseasonal $\bar{u}$ variability; hence, the seasonal cycle and interannual variability were removed from the dataset before applying EOF analysis. This was accomplished by subtracting each winter's mean from each winter's daily data (hence, removing the interannual variability), then removing the seasonal cycle from each winter by applying a fifth-order polynomial to each of the six 120-day winter time-series. From 23 latitudinal $\bar{u}$ values, 23 eigenvectors were computed. In this manner, dominant modes of daily $\bar{u}$ wind variability are isolated for the region from 48.1°N to 48.1°S during the six winters.

3. Zonal wind index

Figure 1 depicts the first four intraseasonal $\bar{u}$ eigenvectors (E1–E4) and their percent variance contributions to the total intraseasonal $\bar{u}$ variance. Based on a significance test for principal components described by Overland and Preisendorfer (1982), the first four eigenvectors in Fig. 1 easily exceed the significance criterion for eigenvectors. The dominant intraseasonal eigenvector E1 contains 26% of the total intraseasonal $\bar{u}$ variance. Eigenvector E2 looks very similar to E1, except it is displaced southward by about 10 deg lat. Moreover, E2 can be shown through lag correlation to be related to E1. Indeed, examination of the E1 and E2 coefficient time series (not shown) indicates that maxima (minima) in E2 lag maxima (minima) in E2 by about 12–15 days for the strongest cycles of both eigenvectors. This is indicative of a stationary and moving component to a single physical phenomena being captured by E1 and E2.

By performing spectral analysis on each winter's time-dependent coefficients associated with the four dominant eigenvectors, then averaging the six winter spectra, it is found that the four dominant $\bar{u}$ EOFs are characterized by variability on the order of 15–35 days (Fig. 2). Note that the long-period end of spectral power is significantly reduced and approaches zero beyond 60 days since seasonal and interannual cycles have been removed from the data prior to performing spectral analysis. Caution should be taken in the interpretation of the spectra in Fig. 2. The contribution of power at various periods is substantially different for individual winter spectra. For example, winters 1974/75, 1977/78 and 1978/79 contribute strongly to a 25–35 day periodicity while winters 1973/74 and 1975/76 contribute most strongly to a 15–17 day periodicity. Hence, there appears to be large interannual variability in the temporal behavior of fluctuations. In general, however, these spectra of $\bar{u}$ variability are consistent with previous Northern Hemisphere zonal wind studies (i.e., 2

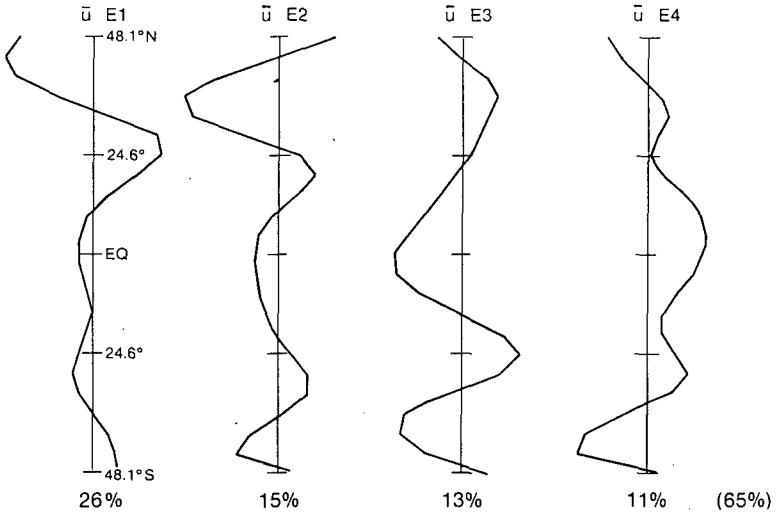

FIG. 1. 200 mb zonally averaged wind normalized eigenvectors, E1 (left) through E4 (right) from 48.1°N (top) to 48.1°S (bottom). Seasonal trend and interannual variability have been removed. Computed from six 120-day winters (1 Nov.–28 Feb.), 1973/74 to 1978/79. Percent $\bar{u}$ variance explained by each eigenvector is shown at bottom.

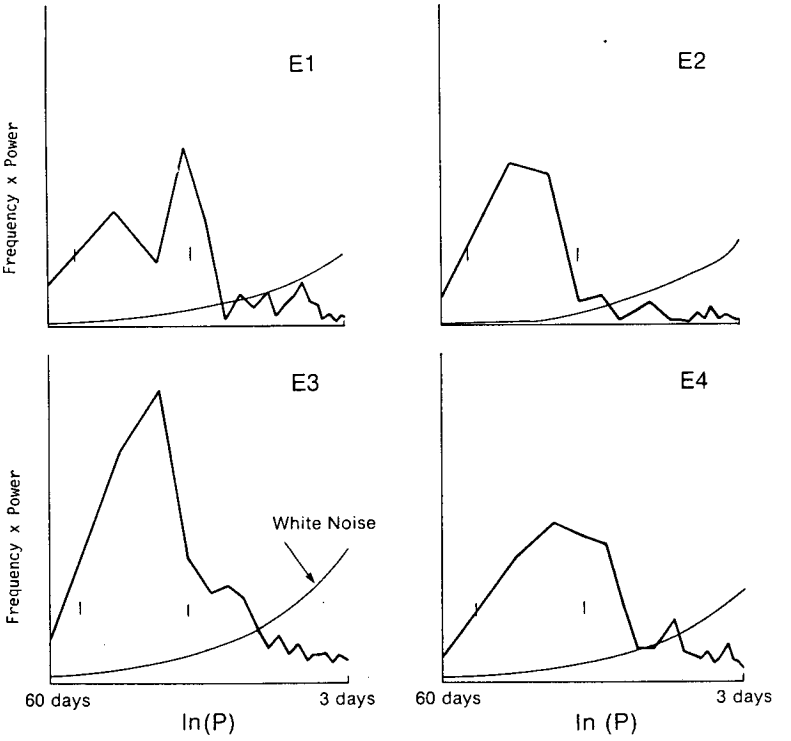

FIG. 2. Six-winter average of frequency × power for the time-dependent coefficients of eigenvectors E1 (top left) through E4 (bottom right). Tick marks at 15 and 35 days indicate the 0.5 power of the low-pass time filter. White noise spectra are shown for each eigenvector.

weeks to 1 month). Significance tests for spectral peaks were not applied. However, accurately resolving cycles with periods longer than 20 days with only 120-day time series is difficult, since so few cycles are sampled over each winter. These spectra are reproduced primarily for the purpose of portraying the result that the majority of $\bar{u}$ variability, regardless of how periodic, is dominated by fluctuations longer than 10 days and shorter than 40 days.

Based on the frequency spectra in Fig. 2, a broad low-pass filter was applied to the $\bar{u}$ time series (see Shanks 1967; Murakami 1980) with 0.5 power at approximately 15 and 35 days, and a peak power of 0.9997 at 27 days. The shape of this filter weights the 25–30 day spectral peak in E1 much more than the 15–17 peak. This was done deliberately, since the 25–30 day cycles in eigenvector E1 display larger amplitude (although less frequent) than the 15–17 day cycles. Also, the E2 eigenvector, which contributes to the following composites, is dominated by 25–30 day oscillations (Fig. 2, top right). The EOF analysis was reapplied to the 15–35 day filtered $\bar{u}$ time series. The four dominant time-filtered $\bar{u}$ eigenvectors are nearly identical to those in Fig. 1, and hence are not shown. Their contributions to the time-filtered variance are also very similar to the variances associated with unfiltered eigenvectors.

The focus is on the dominant time-filtered $\bar{u}$ eigenvector E1, which depicts a mode of variability in which $\bar{u}$ variations at 45°N are out-of-phase with $\bar{u}$ variations near 25°N. This E1 mode is similar to zonal wind variations found in previous studies (e.g., Rosen and Salstein 1983; Branstator 1984; Kidson 1985). In particular, it is very similar to the E2 mode depicted in Rosen and Salstein (1983). Their domain extended from 90°N to 90°S; however, for the mode of interest here, little information about E1 is lost by a truncated analysis at 48.1°N and 48.1°S. Interestingly, the power spectrum associated with Rosen and Salstein's mode 2 is dominated by peaks near 17 and 29 days. This is nearly the same as the spectral results for E1 isolated here (Fig. 2). This $\bar{u}$ E1 pattern was not found during Northern Hemisphere summer, nor in either summer or winter in the Southern Hemisphere (Lyons 1986). Yoden et al. (1987) have isolated a Southern Hemisphere $\bar{u}$ mode of variability which occurs predominantly south of 45°S. Their mode fluctuates on fairly long (months) time scales, and bares little resemblance to the Northern Hemisphere E1 mode described here.

The E1 time-dependent coefficient time series (Fig. 3) is used as the primary composite index. Clearly evident are zonal wind oscillations on a time scale of about 25–35 days occurring during some of the six winters (in particular, 1974/75, 1977/78, and 1978/79). The 15–17 day oscillations prominent in winters

1973/74 and 1975/76 have been significantly damped (~0.5) by the filter, and hence appear weak in Fig. 3. Note that the time coefficient for any day (Fig. 3) multiplied by the E1 eigenvector (Fig. 1) will produce the sign and normalized magnitude of the anomaly-$\bar{u}$ meridional profile for that day.

As suggested by the spectra in Fig. 2, the periodicity of prominent $\bar{u}$ oscillations shown in Fig. 3 generally appears to be shorter than oscillations associated with the 40–50 day tropical wind/convection cycle. However, some of the $\bar{u}$ oscillations depicted in Fig. 3 (e.g., during 1977/78 and 1978/79) have periods near 35 days which overlap with the broadly defined 30–60 day tropical oscillation. Consequently, it is dangerous to conclude, based only on spectral characteristics, that they are two separate oscillations. To examine whether the $\bar{u}$ E1 time series (Fig. 3) is significantly correlated with the tropical 40–50 day oscillation, a concurrent tropical index was obtained for the three winters, 1976–77 through 1978–79. (This period contains six of the nine cycles used in subsequent composites). The tropical index is defined by the dominant EOF associated with 40–50 day 250 mb and 850 mb winds over the global tropics, computed over the period 1976 to 1985.

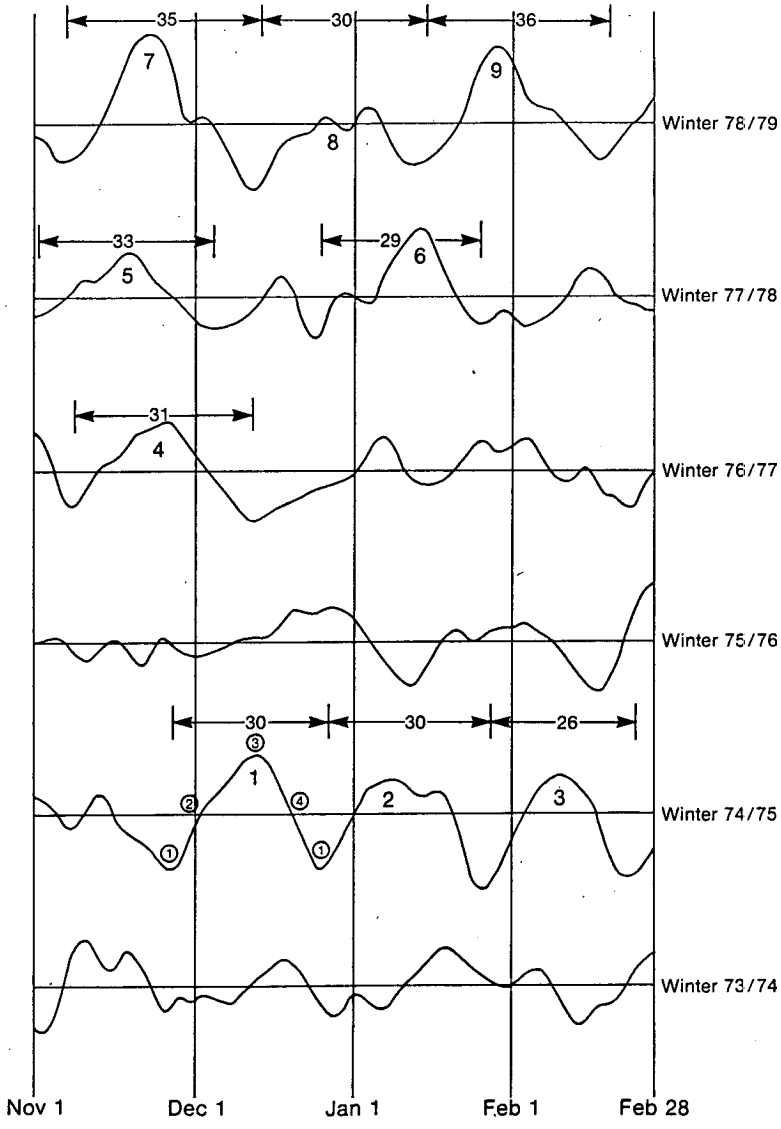

FIG. 3. Normalized time-dependent coefficients for 15–35 day filtered $\bar{u}$ eigenvector E1: 1 Nov. (left) through 28 February (right), 1973/74 (bottom) through 1978/79 (top). Large numbers correspond to nine dominant cycles used in composites. Small circled numbers correspond to composite categories 1 to 4 for cycle 1. The interval and period (days) of each of the nine dominant cycles are marked with arrows and numbers, respectively.

Index values, available at 5-day intervals, were obtained from the University of Wisconsin and are described in Anderson (1987). The contemporaneous correlation between both 5-day interval time series was 0.15, which is not significant even under the most lenient assumptions—that the populations are normal with zero correlation. Lag correlations with $\bar{u}$ E1 and the tropical index separated by 5, 10, 15 and 20 days failed to produce any significant correlations (all correlations were less than 0.31), at least for this short data sample which included 72 5-day interval pairs. Consequently, it appears that the subtropical/middle latitude $\bar{u}$ E1 oscillation is not strongly related to the tropical oscillation during the interval tested.

Nine prominent $\bar{u}$ cycles are defined in the E1 time series; they are boldly numbered in Fig. 3. They were chosen based on the criterion that the difference between the maximum and minimum points of an approximate 30-day cycle exceeds two standard deviations (where the standard deviation was computed over all six 120-day winter time series in Fig. 3). From these nine cycles, $\bar{u}$ wind anomalies at each latitude were composited, by averaging $\bar{u}$ winds occurring during four categories within each of the nine cycles. Composite category 1 corresponds to an E1 time-coefficient minimum, category 2 corresponds to an E1 time-coefficient zero point (increasing), category 3 corresponds to an E1 time-coefficient maximum, and category 4 corresponds to an E1 time-coefficient zero point (decreasing). Composite categories 1 to 4 are indicated in Fig. 3 by circled numbers for cycle number 1. Definition of additional categories gives little added information on the temporal evolution of each cycle.

The time-filtered $\bar{u}$ composite over categories 1–4 (an average period of 31 days) is shown in Fig. 4. Clearly evident is a systematic temporal sign reversal in zonal wind anomalies at 45° and 25°N, each being out of phase with the other. These fluctuations ($\bar{u}$ anomalies) are on the order of ±3–4 m s^{-1}. Although there is a large standing component to the oscillation, rather obvious is a southward migration of $\bar{u}$ anomalies from 48.1° to 25°N superimposed on the standing oscillation. There is weak southward $\bar{u}$ propagation also evident from the equator to 40°S, and weak northward $\bar{u}$ propagation evident between the equator and 20°N. A detailed description of the meridional propagation of $\bar{u}$ anomalies for both the Northern and Southern hemispheres is given in Lyons (1986). The cause for the meridional propagation of $\bar{u}$ anomalies is not known.

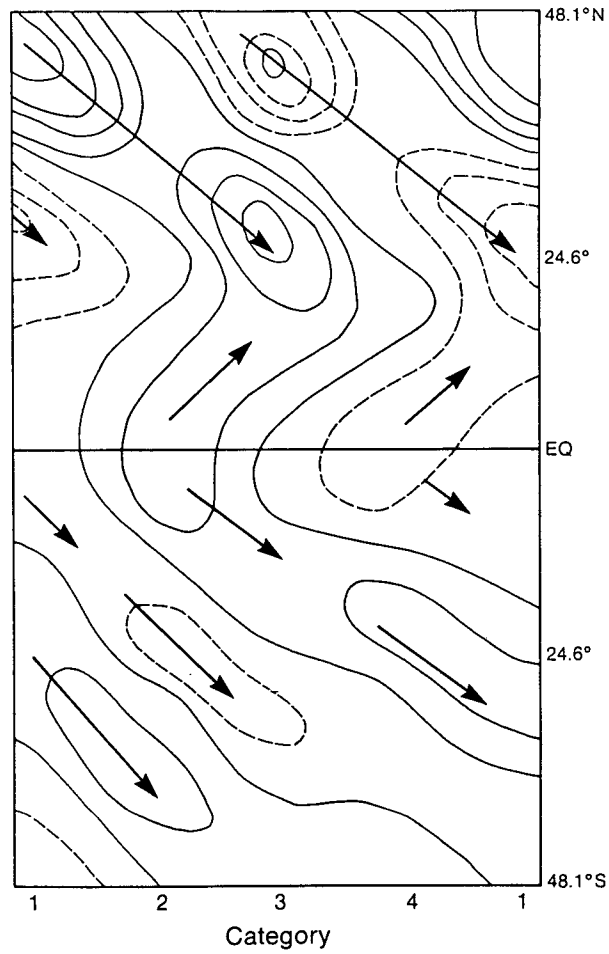

FIG. 4. A 200 mb low-pass filtered $\bar{u}$ composite from 48.1°N (top) to 48.1°S (bottom). Category 1 (left) through category 4 (right). Contour interval is 1 m s^{-1}. Dashed lines indicate negative values. The time interval for one complete cycle is about 30 days.

4. Zonal/eddy relationship

To isolate the time transient eddy relationship to $\bar{u}$ oscillations associated with eigenvector E1 (Fig. 4), daily 200 mb u and v winds were time filtered at each grid point over the domain from 48.1°N to 48.1°S, 180°W–180°E, for each of the six winters. The identical filter as described in section 3 was applied. Composites of time-filtered u and v winds over each of the nine $\bar{u}$ cycles were generated. Composite categories 1 to 4 for u and v appear in Figs. 5a–d, respectively, for the region from 180°W to 180°E, and from the equator to 48.1°N. Composites using unfiltered u, v winds reproduce all of the following results; however, unfiltered fields are noisier. Composite fields for the Southern Hemisphere are not displayed. Although weak $\bar{u}$ anomalies were found over the Southern Hemisphere (Fig. 4), only very small and nonsystematic u, v composite amplitudes were found there from the E1 composite. Hence, there does not appear to be a clear-cut relationship between zonal ($\bar{u}$) oscillations and eddies in the Southern Hemisphere, at least associated with E1 over the domain extending to 48.1°S.

Categories 1 and 3 (E1 extrema) are associated with large zonally oriented u wind anomalies out of phase between 45° and 25°N. These regional u wind anomalies contribute to the $\bar{u}$ anomalies associated with the

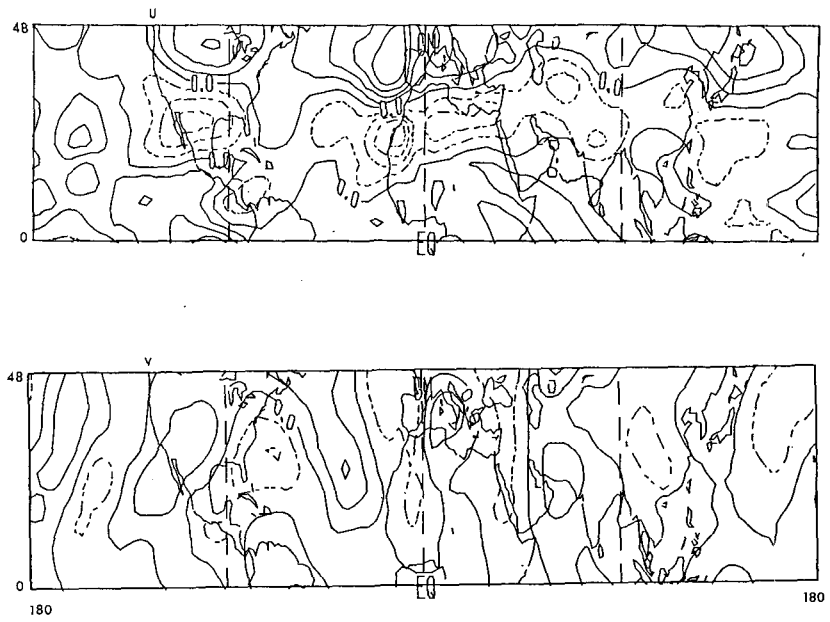

FIG. 5a. Composite category 1 of 15–35 day filtered u (top) and v (bottom). Domain is from 180°W to 180°E and 48.1°N to the equator. Contour interval is 2 $m \cdot s^{-1}$ for both u and v. Dashed lines indicate negative values.

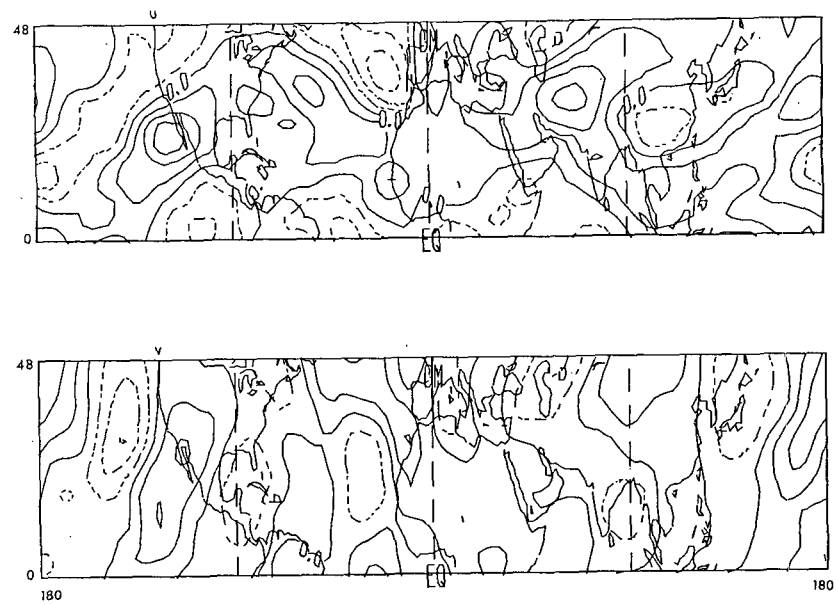

FIG. 5b. As in (a), except for category 2.

index (Fig. 4). Simultaneously, however, meridional (v) wind anomalies are very small. Consequently, category 1 and category 3 fields are dominated by u wind anomalies, which are nearly opposite in sign and magnitude between the two categories. Conversely, composite categories 2 and 4 (E1 inflection points) display large and systematic meridional wind anomalies, particularly strong over the eastern Pacific, North America, and the central Atlantic. The u wind anomalies over these regions are also large, but unlike categories 1 and 3, during which times u wind anomaly patterns were primarily zonally oriented, the patterns display marked

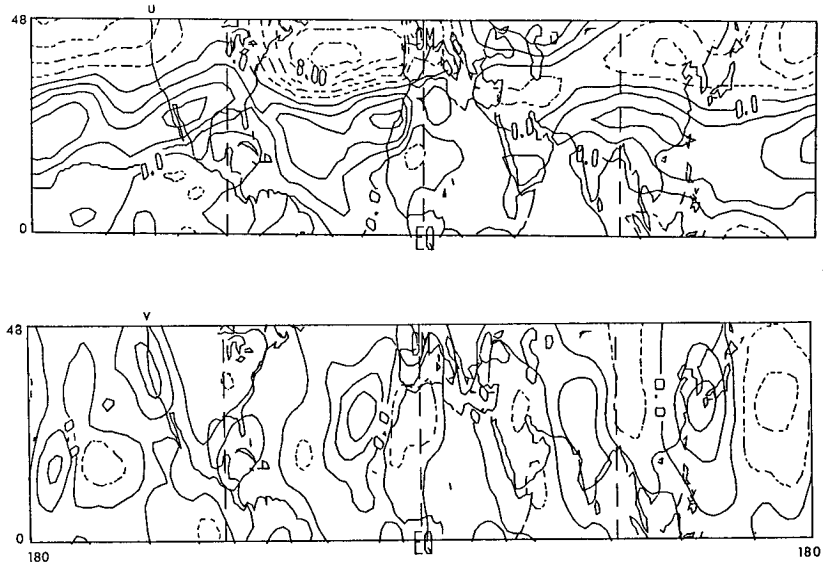

FIG. 5c. As in (a), except for category 3.

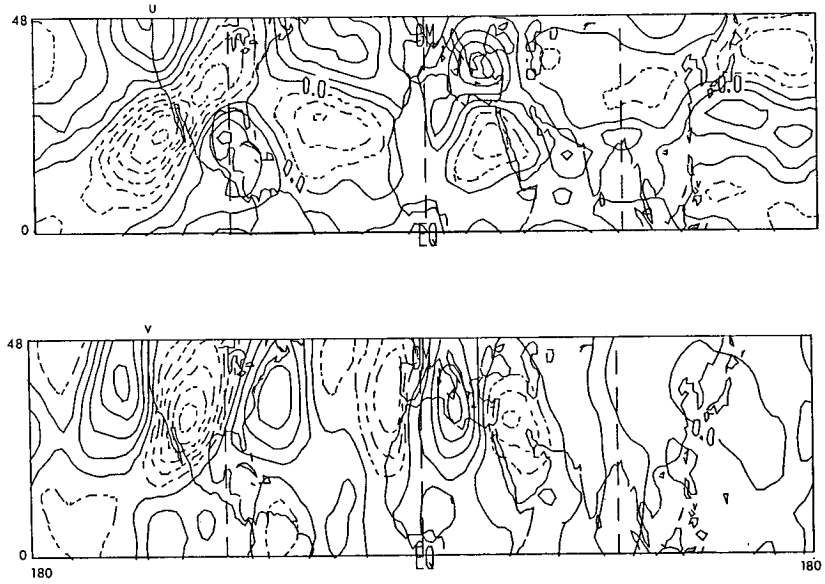

FIG. 5d. As in (a), except for category 4.

meridional structure. As a consequence, zonally averaged u is small during categories 2 and 4 (consistent with Fig. 4).

Hence, during peak positive and negative phases of the E1 zonal wind index, global eddy anomalies are associated primarily with zonally oriented u wind anomaly patterns, which are most pronounced from 180°W–0°. On the other hand, during the zero phases of the E1 zonal wind index, and apparently during the time either positive or negative $\bar{u}$ anomalies are moving southward from 48° toward 25°N, meridional eddy activity is greatly enhanced. Consequently, there are transitions between zonal and meridional anomalous circulations between categories 1 and 2 and between categories 3 and 4. No evidence was found which would suggest east–west or north–south propagation of v anomalies. Instead, a localized (180W–0°) amplification of v wind anomalies and meridional distortion of u anomalies occurs during categories 2 and 4, preceded and followed by weak v wind anomalies and zonally oriented u wind anomalies (categories 1 and 3).

These anomalous zonal/meridional circulation

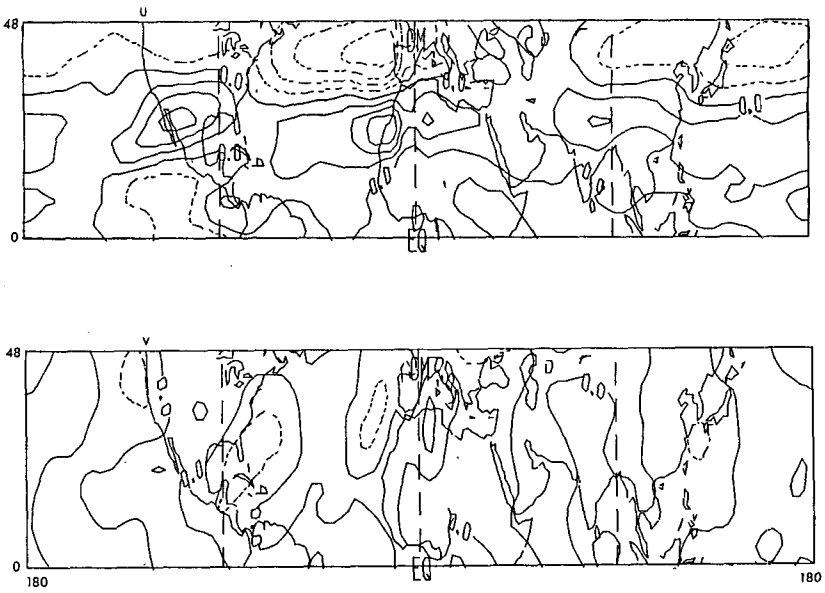

FIG. 6a. As in Fig. 5, except difference fields; 15–35 day filtered composite category 3 minus composite category 1, u (top), v (bottom). Contour interval is 4 m s^{-1} for both u and v.

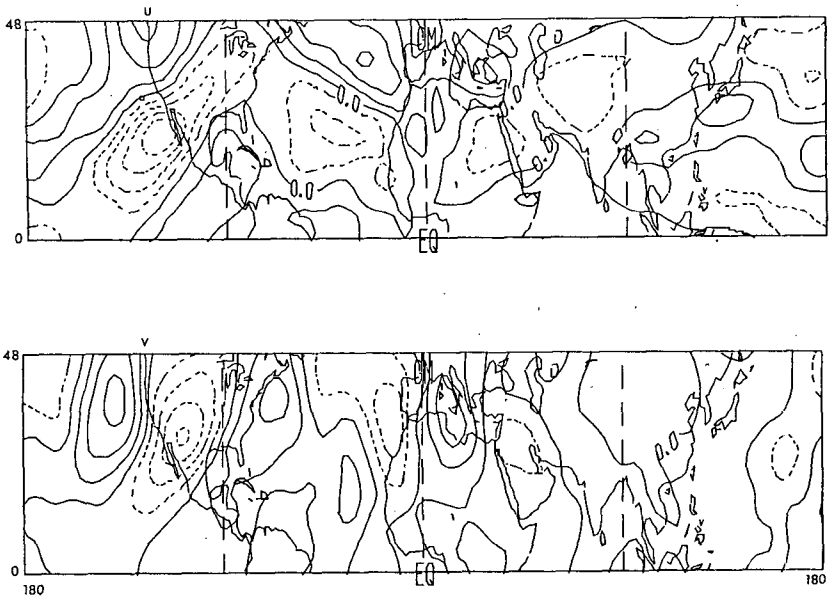

FIG. 6b. As in (a), except for composite category 4 minus composite category 2.

changes are shown clearly in Figs. 6a and 6b, where difference fields between categories 3 and 1 and categories 4 and 2, respectively, are shown. The primary contribution to $\bar{u}$ anomalies during categories 1 and 3 are from u anomalies in the Pacific, North America, and Atlantic sectors. The u wind anomalies over central Asia are small, although larger during category 1 than during category 3.

Interestingly, the v anomalies during categories 2 and 4 are largest over the regions where u wind anomalies during categories 1 and 3 are largest; viz., 180°W to 0°. The dominant features associated with category 4 minus category 2 (Fig. 6b) are a series of anomalous cyclones/anticyclones extending from 160°W to 60°E, maximum over North America. For example, the western United States and the central Atlantic display

anomalous anticyclones while the eastern Pacific and the eastern United States display anomalous cyclones during category 4. These anomaly circulations are very similar to a situation of blocking over the western United States and the central Atlantic. Opposite circulation anomalies dominate during category 2.

The above results are reproduced nearly identically at the 500 mb level (not shown); however, most of the anomaly magnitudes are roughly 80% of those at 200 mb. Hence, both the zonal wind anomalies and the eddy anomalies show a nearly equivalent barotropic character between 200 mb and 500 mb.

5. Discussion

The cause of the zonal/eddy oscillation isolated here has not been addressed and may be difficult to isolate diagnostically. Possible candidates include barotropic instability of the mean flow (multiple equilibrium states existing in the atmosphere and tropical convectively forced anomalies). Particularly intriguing is the similarity between the eddy anomalies over North America depicted in categories 2 and 4 (Fig. 6b, bottom), and wintertime orographically forced stationary eddies generated by general circulation models (GCMs) and linear GCMs (see Manabe and Terpstra 1974; Nigam et al. 1988). For example, Figs. 4e–f in Nigam et al. (1988) display the stationary 300 mb winter mean meridional wind anomalies associated only with orographic forcing, for both linear GCM and full GCM simulations. Although these simulations contain v anomalies associated with the entire Northern Hemisphere mountains, it will suffice here to say that the anomalies from the Gulf of Alaska to 0° long are primarily associated with the Rocky Mountains.

One could envision that a strengthening and weakening (as compared to the winter average) of the model simulated meridional wind patterns could produce stationary time-transient meridional wind anomalies similar to those isolated in Figs. 5b and 5d, or more clearly those shown in Fig. 6b, bottom (the sign of the v anomalies being reversible). The longitudinal phase locking of the eddies over North America in categories 2 and 4 are consistent with this scenario; i.e., these eddy anomalies which develop, decay and redevelop with opposite sign from category 1 to 4 are consistent with stationary, time-transient anomalies. This could explain the absence of the oscillation in the Southern Hemisphere, where orographically forced waves (away from Antarctica) have been shown to be small. The absence of the oscillation over the Northern Hemisphere subtropics/middle latitudes in summer would also be anticipated, since the westerlies shift far north in summer and do not interact with the widest and highest sections of the Rockies and Himalayas. This could also explain why eddy anomalies in categories 2 and 4 are small in the vicinity of Tibet (a major source of orographically forced eddies in the winter mean circulation) since the zonal wind oscillation over Asia associated with E1 is very small compared to the Rocky Mountain region (Fig. 6a, top). Zonal wind anomalies over Tibet were larger during category 1 as compared to category 3 (Fig. 5a and 5c, top). Coincidently, category 2 (Fig. 5b) does show weak eddy anomalies over and downwind of Tibet, which are absent in category 4 (when zonal wind anomalies there, including category 3, are nearly zero). Although very weak, the phase and wavelength of the category 2 eddy anomalies over Tibet and Japan (Fig. 5b, bottom) show some similarity to GCM modeled winter mean orographically forced waves associated with the Tibetan massif (see Nigam et al. 1988).

6. Conclusion

We have isolated a wintertime Northern Hemisphere subtropical/middle latitude zonal wind oscillation with a period of about 15–35 days. It is absent in summer and was not found in summer or winter in the Southern Hemisphere. It has small amplitude along the equator, tends to oscillate with a period shorter than or on the short end of the 30–60 day time scale, and is not significantly correlated with a 40–50 day tropical index (at least during the winters 1976/77 through 1978/79). Hence, it does not appear that this $\bar{u}$ oscillation is directly related to the tropical 40–50 day oscillation. Between 500 and 200 mb, its structure is nearly barotropic. Interannual changes in the frequency, strength and persistence of this oscillation are significant. However, for winters which do exhibit large zonal wind oscillations, a systematic and well-defined relationship exists between the anomalous zonal wind oscillations and anomalous eddy oscillations. The peak positive and negative phases of the $\bar{u}$ wind anomalies are characterized by 1) very small meridional wind anomalies, and 2) zonally oriented u wind anomaly patterns which are strongest from 180°W to 0° with an opposite sign between negative and positive phases. Conversely, zero phases of the $\bar{u}$ wind anomalies are characterized by 1) large meridional wind anomalies with an opposite sign between increasing and decreasing zonal wind index phases, 2) u wind anomaly patterns with significant meridional structure, and 3) largest v anomalies observed from 180°W to 0°, which show no tendency to propagate east–west or north–south.

Although the cause of this oscillation is unknown, these results give additional evidence for a zonal/eddy relationship over subtropical and middle latitudes of the Northern Hemisphere during winter.

Acknowledgments. Thanks to Jay Rosenthal, a portion of this work was supported by the Pacific Missile Test Center, Geophysics Division, Point Mugu, California. Thanks also to Dr. J. Anderson, who gave many useful suggestions and furnished the tropical time series

used in the time-series correlation, and to Drs. Isaac Held, Richard Rosen and James McGuirk for helpful comments and suggestions.

REFERENCES

Anderson, J. R., 1987: Some diagnostic results concerning the tropical 40–50 day oscillation. *Proc. Twelfth Annual Climate Diagnostics Workshop,* U.S. Dept of Commerce, 102–105.

——, and R. D. Rosen, 1983: The latitude-height structure of 40–50 day variations in atmospheric angular momentum. *J. Atmos. Sci.,* **40,** 1584–1591.

Branstator, G., 1984: The relationship between zonal mean flow and quasi-stationary waves in the midtroposphere. *J. Atmos. Sci.,* **41,** 2163–2178.

Defant, F., and H. Taba, 1958: The strong index change period from January 1 to January 7, 1956. *Tellus,* **10,** 225–242.

Kidson, J. W., 1985: Index cycles in the Northern Hemisphere during the Global Weather Experiment. *Mon. Wea. Rev.,* **113,** 607–623.

Krishnamurti, T. N., and D. Subrahmanyam, 1982: The 30–50 day mode at 850 mb during MONEX. *J. Atmos. Sci.,* **39,** 2088–2095.

Knutson, T. R., and K. Weickmann, 1987: 30–60 day atmospheric oscillations: Composite life cycles of convection and circulation anomalies. *Mon. Wea. Rev.,* **115,** 1407–1436.

La Seur, N. E., 1954: On the asymmetry of the middle-latitude circumpolar current. *J. Meteor.,* **11,** 43–57.

Lau, K.-M., and P. H. Chan, 1985: Aspects of the 40–50 day oscillation during the northern winter as inferred from outgoing longwave radiation. *Mon. Wea. Rev.,* **113,** 1889–1909.

——, and ——, 1986: Aspects of the 40–50 day oscillation during the northern summer as inferred from outgoing longwave radiation. *Mon. Wea. Rev.,* **114,** 1354–1367.

Lyons, S. W., 1986: Observed modes of vacillation in upper tropospheric zonally averaged global zonal winds during winter and summer. *Preprints, Second International Conference on Southern Hemisphere Meteorology.* Amer. Meteor. Soc., 192–195.

Madden, R. A., and P. R. Julian, 1971: Detection of a 40–50 day oscillation in the zonal wind in the tropical Pacific. *J. Atmos. Sci.,* **28,** 702–708.

Manabe, S., and T. B. Terpstra, 1974: The effects of mountains on the general circulation of the atmosphere as identified by numerical experiments. *J. Atmos. Sci.,* **31,** 3–42.

McGuirk, J. P., and E. R. Reiter, 1976: A vacillation in atmosphere energy parameters. *J. Atmos. Sci.,* **33,** 2079–2093.

Murakami, T., 1980: Empirical orthogonal function analysis of satellite-observed outgoing longwave radiation during winter. Part I. Long-period (15–30 day) oscillations. *Mon. Wea. Rev.,* **109,** 408–426.

——, and T. Nakazawa, 1985: Tropical 45-day oscillations during the 1979 Northern Hemisphere summer. *J. Atmos. Sci.,* **42,** 1107–1122.

——, L. Chen, A. Xic and M. Shrestha, 1986: Eastward propagation of 30–60 day perturbations as revealed from outgoing longwave radiation data. *J. Atmos. Sci.,* **43,** 961–971.

Namias, J., 1947: The index cycle and its role in the general circulation. *J. Meteor.,* **7,** 130–139.

Nigam, S., I. M. Held and S. W. Lyons, 1987: Linear simulation of the stationary eddies in a GCM. Part II: The "mountain" model. *J. Atmos. Sci.,* **45,** 1433–1452.

Overland, J. E., and R. W. Preisendorfer, 1982: A significance test for principal components applied to a cyclone climatology. *Mon. Wea. Rev.,* **110,** 1–4.

Riehl, H., J. C. Yeh and N. La Seur, 1950: A study of variations of the general circulation. *J. Meteor.,* **7,** 181–194.

Rosen, R. D., and D. A. Salstein, 1983: Variations in atmospheric angular momentum on global and regional scales and the length of day. *J. Geophy. Res.,* **88,** 5451–5470.

Shanks, J. L., 1967: Recursion filters for digital processing. *Geophysical,* **32,** 33–51.

Wallace, J. M., and D. S. Gutzler, 1981: Teleconnections in the geopotential height field during the Northern Hemisphere winter. *Mon. Wea. Rev.,* **109,** 784–812.

Weickmann, K. M., 1983: Intraseasonal circulation and outgoing longwave radiation modes during Northern Hemisphere winter. *Mon. Wea. Rev.,* **111,** 1838–1858.

Winston, J. S., and A. F. Krueger, 1961: Some aspects of a cycle of available potential energy. *Mon. Wea. Rev.,* **89,** 307–318.

Yasunari, T., 1980: A quasi-stationary appearance of 30 to 40 day period in the cloudiness fluctuations during the summer monsoon over India. *J. Meteor. Soc. Japan,* **58,** 225–229.

Yoden, S., M. Shiotani and I. Hirota, 1987: Multiple planetary flow regimes in the Southern Hemisphere. *J. Met. Soc. Japan,* **65,** 571–585.